A High-Throughput Screening Assay for NKCC1 Cotransporter Using Nonradioactive Rubidium Flux Technology

Sikander Gill,[1] Rajwant Gill,[1] Yang Wen,[2] Thilo Enderle,[2] Doris Roth,[2] and Dong Liang[1]

[1]Aurora Biomed Inc., Vancouver, Canada.
[2]Roche Innovation Center Basel, Hoffmann–La Roche, Basel, Switzerland.

ABSTRACT

A high-throughput screening (HTS) assay was developed for cotransporter, NKCC1, which is a potential target for the treatment of diverse disorders. This nonradioactive rubidium flux assay coupled with ion channel reader series provides a working screen for this target expressed in human embryonic kidney (HEK) cell line. An eightfold window of detection was achieved with the optimized assay. This new functional assay offered a robust working model for NKCC1 in determining reliable and concordant rank orders of the test compounds supporting its sensitivity and specificity. The robustness of manual assay indicated by Z' of 0.9 qualified its amenability to automation. The Z' of 0.7 was displayed by automated assay employed in high-throughput screening of compound libraries against this target. Being electrically neutral, the NKCC1 screening is difficult to achieve by both manual and automated electrophysiological techniques. These techniques, although considered gold standard, suffer from their inherent problems of being too slow to be in high-throughput format and with high running costs. In addition to being a functional assay for NKCC1, it is nontoxic as compared with thallium flux assay, which is prone to generate high number of false-positive/false-negative rates because of its innate fluorescence issues.

Keywords: HTS, flux assay, rubidium, cotransporter, compound screening, Ion Channel Reader

INTRODUCTION

The cotransporter NKCC1 is an intrinsic membrane protein that actively transports Na^+, K^+, and Cl^- across the cell membrane.[1,2] It moves each of these ions in the same direction leading to electroneutrality by maintaining stoichiometry of $1Na^+:1K^+:2Cl^-$. As NKCC1 is electrically neutral, its monitoring is difficult to achieve by patch clamping, which is considered a gold standard technique and thus screening is not feasible with this technique. However, high-throughput screens (HTS) have been reported for this target with fluorescence-based thalium (Tl^+) or pH-sensitive fluorescence-based NH_4 influx.[3–6] But Tl^+ screen suffers from toxicity and artifacts leading to high false-positive/false-negative rates. In this assay, Tl^+ has been used as a tracer for K^+ and its influx into cells is measured with the Tl^+-sensitive fluorescent dye. However, large concentrations (mM) of the highly toxic thallium, and cell toxicity caused by Cl^--free buffer conditions necessary to generate a robust assay read-out, are a matter of concern.[7] Moreover, the optical (fluorescence) properties of the unknown test compounds during screening of compound libraries may skew the data and thus lead to high false positive/negative rates.[7,8] In addition, the unknown test compound may also modify the fluorescence signal because the principle of this method is based on the sensitivity to Tl^+. Pyrilamine is a fine example from fluorescence-based human *ether-à-go-go* related gene (hERG) screen, wherein this compound has no detectable fluorescence of its own but results in false-negative rates.[9] The endogenous off-target pathways like Na^+,K^+-ATPase from the native cells expressing the target could also interfere with the Tl^+ influx, which will cause a higher false-positive or false-negative hit rate.[8] An alternative fluorescence-based approach using NH_4 influx with NKCC1 measured with a pH-sensitive fluorescence has also been found undesirable because of cytotoxicty.[6] Another HTS performed for this target using rubidium ($^{86}Rb^+$) assay is undesirable because of concerns about radiation hazard[4–9]

This cotransporter plays a key role in the regulation of neuronal excitability, cell volume homeostasis, body salt levels, and blood pressure.[10–12] However, the profound defects in the gene coding NKCC1 alter its pharmacokinetic and dynamic activity profiles, deeming it as a potential target for the treatment of diverse disorders.[1,2,13,14] The electroneutral transport of ions through this target across the membrane is inhibited by several compounds, including bumetanide and furosemide.[2,14]

A suitable HTS for electroneutral transporters is offered by nonradioactive Rb^+ flux assay. Over the decade, the Rb^+ flux assay has emerged as a powerful tool in the field of drug discovery wherein diverse ion channels and cotransporters involving K^+, Na^+, and Cl^- have been targeted.[15–23] This method employs Rb^+ as a tracer or surrogate ion for K ion.[15–21] Since the NKCC1 transports Na^+, K^+, and Cl^- ions across the cell membrane, the principle of Rb^+ flux assay was applied to develop a high-throughput screen for lead compounds against this target by using Rb^+ as a tracer for K^+ in the present studies.

MATERIALS AND METHODS

1. Procurement of chemicals, drugs, and instruments: Molecular biology grade chemicals including antibiotics, tissue culture media, doxycycline, digoxin, and other compounds were purchased from Sigma-Aldrich Co (St-Louis, MO). The human embryonic kidney (HEK) cell culture media, fetal calf serum, and media supplements were obtained from Invitrogen Canada, Inc. (Mississauga, Canada). The Ion Channel Reader (ICR) series ICR8000™ and ICR12000™ (Aurora Biomed, Inc., Vancouver, Canada) were used for detecting intracellular concentration of Rb^+ in the cell lysates.

2. Preparation of multiwell plate with cell culture:
   (a) The cell line inducibly expressing NKCC1 was cultured in the T75 flask at about 95% confluency in a humidified 37°C/5% CO_2 incubator for 24 h.
   (b) The untrypsinized cells were scrapped off the surface and the resulting cell suspension after gentle trituration was collected into a conical sterile centrifuge tube (15 mL).
   (c) After centrifugation at 200 g for 5 min, the cell pellet was resuspended in prewarmed fresh growth medium (normal medium or induction medium) after discarding the spent medium. In case of inducing the NKCC1 gene, the culture medium was supplemented with doxycycline (1 μg/mL) 24 h before performing the assay.
   (d) The cell suspension was verified under a microscope to ensure the cells were detached and clumps completely dispersed. The number of cells was determined using a standard operating procedure of hemocytometer.
   (e) The appropriate cell density was adjusted (1.1×10^7 cells/20 mL) by adding prewarmed growth medium to the cell suspension. Then 200 or 75 μL of the cell suspension thus generated was dispensed into a sterile 96- or 384-well plate, respectively.
   (f) The 96- or 384-well plate with seeded cell suspension was placed in a humidified 37°C/5% CO_2 incubator for 24 h to achieve ~100% confluency.

3. Steps of the assay protocol: All the steps of the assay were performed at room temperature unless otherwise stated (Table 1).

4. Calculations: The Rb^+ influx at any given point of time/concentration represented by (F) is defined as follows[15]:

$$F = [Rb^+_{(intracellular)}] \tag{1}$$

The effect (E) of a compound is defined as follows:

$$E = \left[\left(F_{compound} - F_{basal\ buffer} \right) / \left(F_{activation\ buffer} - F_{basal\ buffer} \right) \right] \times 100, \tag{2}$$

where $F_{compound}$, $F_{basal\ buffer}$, and $F_{activation\ buffer}$ are the Rb^+ influx in the presence of test compound in activation buffer, basal buffer, and activation buffer, respectively.

The quality of the assay performance was evaluated by calculating Z′ as follows.[24]

$$Z' = 1 - \left[3 \times \left(SD_p - SD_n \right) / \left(M_p - M_n \right) \right], \tag{3}$$

where SD_p represents the standard deviations of the positive control (in the presence of activator) and SD_n represents the standard deviations of the negative control (in the absence of activator). M_p and M_n represent the means of positive control and negative control, respectively.

RESULTS AND DISCUSSION

The tracer ion flux assays employing atomic absorption spectrophotometry-based ICR series have been recognized as powerful HTS tools for screening compound libraries for various ion channel and cotransporter targets.[15–23] In the present studies, Rb^+ was used as a tracer in the attempt to develop an HTS assay for NKCC1. The assay was designed in a high-throughput format. During optimization, a significant response was observed from each of the parameters applied and it emerged with high temporal resolution.

Rb^+ as Tracer

The nonradioactive Rb^+ flux assay is supported by the fact that the hydrated Rb^+ has diameter close to K^+, thus it could be employed as a surrogate ion to replace K^+ in the screening assays. Moreover, Rb^+ being absent in biological systems, its signal from the assay could not suffer from background noise, and the Rb^+ flux is measurable by ICR8000/ICR12000 technology.[15–21] The NKCC1 being intrinsic membrane proteins and actively transporting Na^+, K^+, and Cl^- across the cell membrane suggested the feasibility of developing an HTS with Rb^+ influx through this target.

In this assay, we used the buffers of ionic compositions free from Rb^+ except the influx buffer that contained Rb^+ in place of K^+. The absence of K^+ from the influx buffer was necessary

Table 1. Steps of the Assay Protocol

No.	Step	Description
1	Preparation of dose stock of the test compounds	The eight test doses of a test compound were prepared as 100× of the desired dose range. From each dose stock, 2 μL was used to mix with assay buffer (198 μL) per well, resulting in 1× strength. A 100× stock dose was also prepared for ouabain or digoxin at 100 mM. The cell plate was removed from the incubator and checked under microscope for ∼100% confluency and morphology of the cells.
2	Hypotonic incubation	Culture medium in the 96-well plate was replaced with 200 μL hypotonic buffer (67.5 mM sodium gluconate, 2.5 mM potassium gluconate, 15 mM HEPES, 5.0 mM glucose, 1.0 mM $MgSO_4$, 1.0 mM $CaCl_2$, 1.0 mM Na_2HPO_4, and 1 mM NaH_2PO_4) by using a 12 channels pipettor and the plate was incubated at room temperature for 60 min from the Rb^+ influx step.
3	Preparation of test dose regime	The dose regime was prepared in two clear polystyrene, nonsterile 96-well plates designated as plate A and plate B, respectively, in a matching format to run $n=3$ of each dose by dispensing 2 μL at the bottom of the corresponding wells of the plate column wise starting with weakest dose in the A row of the plate. In both the plates, 2 μL of ouabain or digoxin was also added to all the test wells.
4	Preincubation with the test compounds	A total of 198 μL of the hypotonic solution was added to plate A, 15 min before the end of the hypotonic incubation step. The solution was mixed twice. It was followed by replacement of hypotonic solution from the cell plate with 200 μL buffer from plate A. The cell plate was incubated at 10 min from the Rb^+ influx step. It was followed by addition of 198 μL of Rb^+ influx buffer (135 mM NaCl, 7.5 mM RbCl, 15 mM HEPES, 5 mM glucose, 1 mM $MgSO_4$, 1 mM $CaCl_2$, 1 mM Na_2HPO_4, and 1 mM NaH_2PO_4) into the wells of plate B. The solution was mixed twice.
5	Rb^+ influx	At the end of 60 min preincubation step, the buffer from the cell plate was replaced with 200 μL from plate B. The Rb^+ influx was allowed for 2 min.
6	Wash steps	The cell plate was washed to remove Rb^+ by replacing the solution in the assay plate with 200 μL of the wash buffer (135 mM NaCl, 7.5 mM RbCl, 15 mM HEPES, 5 mM glucose, 1 mM $MgSO_4$, 1 mM $CaCl_2$, 1 mM Na_2HPO_4, and 1 mM NaH_2PO_4). The wash step was repeated four times.
7	Lysis buffer	The wash buffer was replaced with 180 μL of lysis buffer (1% NP-40, CAS 9016-45-9) followed by pipette mixing (2×) to ensure lysis of cells.
8	ICR readout and data analysis	The samples from the cell lysate plate were analyzed for Rb^+ on the ICR8000™ followed by ICR12000™ by autoinjection of 100 and 30 μL, respectively, of the sample by employing autosampler. This was followed by autoinjection of 200 μL of ICR analysis solution. The data were analyzed on Xlfit3.0 for IC_{50} determinations.

Step Notes

1. The assay reagents were reduced to 50 μL for the 384-well plate.
2. Cell plate may be checked under microscope before performing lysis step of the assay to observe cell loss, if any.
3. The volume of the lysis buffer can be 110 or 75 μL for analysis by ICR8000 or ICR12000, respectively. Accordingly, the RbCl concentration in the Rb influx buffer can be adjusted to the analytical range of the Rb^+ on the respective ICR instrument.

to avoid its competition with Rb^+ in the assay. Importantly, this also implies that this assay could be carried out in non-toxic and low salt concentration buffers with normal chloride and other cation concentrations, which may be a limitation on some fluorescent-based assays.[3–5,7–9]

Characterization of the HEK Cell Model

Efforts were made to assess the feasibility of this assay with HEK cells expressing the NKCC1. The doxycycline-induced cells cultured in a 96-well plate were tested for Rb^+ influx under two conditions: presence and absence of preincubation in hypotonic buffer as a Cl^- free buffer followed by activation of NKCC1 for a range of time intervals in the presence of buffer containing Rb^+. To further confirm that the Rb^+ influx would actually be mediated by NKCC1, the effect of its known inhibitor bumetanide was assessed.[2,14] As shown in *Figure 1a*, the Rb^+ influx plateaus after about 7 min of activation during preincubation treatment, which is clearly inhibited by bumetanide (10 μM) as compared with the control involving untreated cells. However, the cells in the absence of hypotonic preincubation step had significantly lower Rb^+ influx, and a part of this influx was sensitive to bumetanide (10 μM). These observations inferred that Rb^+ was also contributed from Na^+,K^+-ATPase in both the hypotonic pretreated and untreated cells, thus this interference needed to be minimized during optimization of the assay. In addition, some bumetanide-
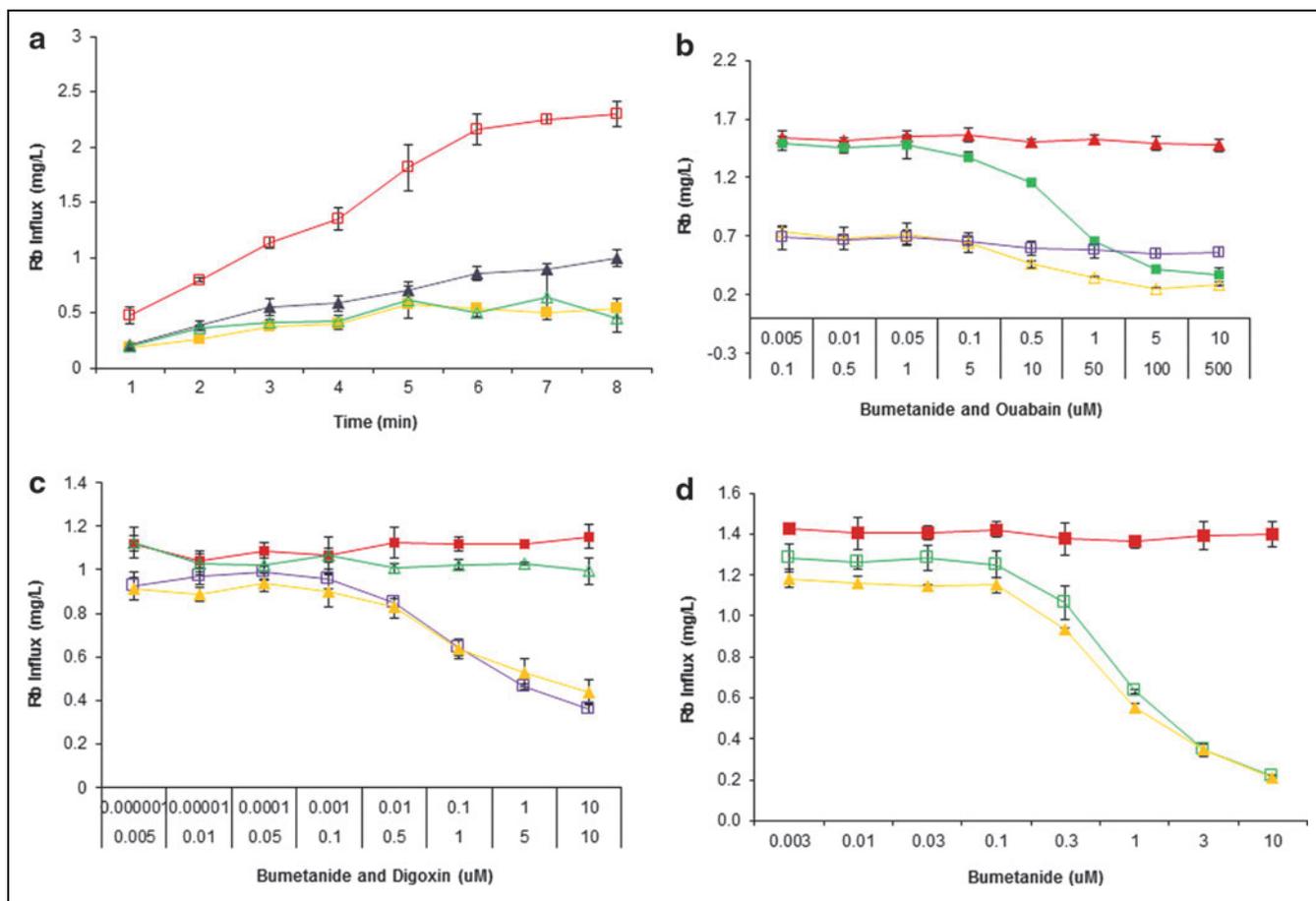
Fig. 1. **(a)** Influx of Rb$^+$ as a function of activation duration: hypotonic preincubation for 60 min in chloride-free medium (□), pre-incubation followed by blocking with bumetanide, 10 μM (■). No preincubation in chloride-free medium (▲) followed by blocking with bumetanide (△). This displays the Rb$^+$ influx contribution by both the Na$^+$,K$^+$-ATPase and NKCC1. **(b)** Comparison of induced and uninduced expression of NKCC1 wherein half of the 96-well plate was induced with doxycycline. Ouabain (*bottom* x-axis) was added to block the Na$^+$,K$^+$ ATPase in induced (△) and uninduced (▲) conditions. Dose response of bumetanide (*top* x-axis) for both the induced (■) and uninduced conditions (□) was evaluated for a duration of 6 min that resulted in four fold window of detection. **(c)** Effect of bumetanide and digoxin on Rb$^+$ influx: activated Rb$^+$ influx (■) in the columns of the assay plate indicated no drifting of signal. It gets inhibited as a dose response of bumetanide (*top* x-axis) in the absence (□) and presence (▲) of 10 μM of digoxin. No significant dose response is displayed by digoxin (△) (*bottom* x-axis), indicating that Na$^+$,K$^+$-ATPase contribution was significantly low at 3 min activation, resulting in 2.6-fold window of detection. **(d)** The activated Rb$^+$ influx (■) in the columns of the assay plate indicates no drifting of signal in comparison with the dose response of bumetanide in the absence (□) and presence (▲) of 10 μM of digoxin while employing cold wash buffer to slow down the kinetics. This treatment elevated the window of detection to 5.9-fold. Error bars represent standard error of $n = 3$ values.

sensitive Rb$^+$ influx by the NKCC1 at basal level was also observed even in the absence of hypotonic pretreatment.

Differentiation of NKCC1 Influx from Na$^+$,K$^+$ ATPase Rb$^+$ Uptake

It is a well-known fact that the electrochemical gradient of Na$^+$ and K$^+$ across the cell membrane is established by Na$^+$,K$^+$-ATPase, an ATP-dependent pump. This pump is also known to uptake Rb$^+$ and is sensitive to cardioglycosides, ouabain, digitoxin, and digoxin.[15] This suggested that the major share of observed Rb$^+$ influx insensitive to bumetanide was medi-

ated by the Na$^+$,K$^+$-ATPase (*Fig. 1a*). Therefore, it was essential to differentiate the Rb$^+$ influx contributed by NKCC1 from that of Na$^+$,K$^+$-ATPase. It could be achieved either by inhibiting or minimizing the Na$^+$,K$^+$-ATPase uptake. For this purpose, ouabain or digoxin, the well-known inhibitors of Na$^+$,K$^+$-ATPase, was employed. In this experiment, half of the 96-well plate was induced with doxycycline. The doxycycline-induced cells were also treated with preincubation in hypotonic buffer to see the effect of induced and uninduced expression of NKCC1 and of Na$^+$,K$^+$-ATPase for a duration of 6 min. Ouabain (1 mM) was added to all the wells of the 96-

Table 2. Profile of Assay Optimization

Experiment	Duration of activation (min)	Basal efflux (%)	Window of detection (fold)	Rb content (mg/L)
Activation duration	7	25	3.9	2.3
Reduced duration	6	23	4.2	2.1
Reduced duration	3	20	2.6	1.2
Cold treatment during wash steps	3	17	5.9	1.4
Increase in extracellular Rb$^+$	3	12	8.4	4.9
Minimize Na$^+$,K$^+$-ATPase interference by reducing duration of activation	2	11	9.5	2.8
Removing interference of Na$^+$,K$^+$-ATPase blocking dose	2	16	6	2.8

well plate. Dose response of bumetanide for both the induced and uninduced conditions was also evaluated. Significantly higher Rb$^+$ influx was observed in case of induced expression than the uninduced cells during 6 min of activation. Interestingly, the Rb$^+$ influx was not completely abolished in the presence of high concentration (10 μM) of bumetanide, suggesting the presence of an endogenous bumetanide-insensitive Rb$^+$ influx. The influx was blocked by bumetanide (10 μM) down to 24%. The Rb$^+$ influx in case of the uninduced cells was sensitive to ouabain and insensitive to bumetanide, whereas in the induced cells, the effects were contrary, displaying sensitivity to bumetanide but not to ouabain (*Fig. 1b*). This experiment resulted in a fourfold window of detection.

With the objective of minimizing the Rb$^+$ uptake by Na$^+$,K$^+$-ATPase, the activation of NKCC1 was reduced from 6 to 3 min. In addition, to minimize the concentration of the Na$^+$,K$^+$-ATPase blocker, a more potent blocker digoxin was used instead of ouabain. The insignificant difference of bumetanide dose response on the induced NKCC1 signal in the presence and absence of Na$^+$,K$^+$-ATPase blocking dose of digoxin suggested that Na$^+$,K$^+$-ATPase contribution was significantly low at 3 min activation. This was also supported by insignificant dose response of digoxin on the induced signal of NKCC1 (*Fig. 1c*). Although interference of Na$^+$,K$^+$-ATPase was minimized in comparison with 6 min activation, it also led to a significant decrease in the window of detection from 4.2- to 2.6-fold (*Table 2*).
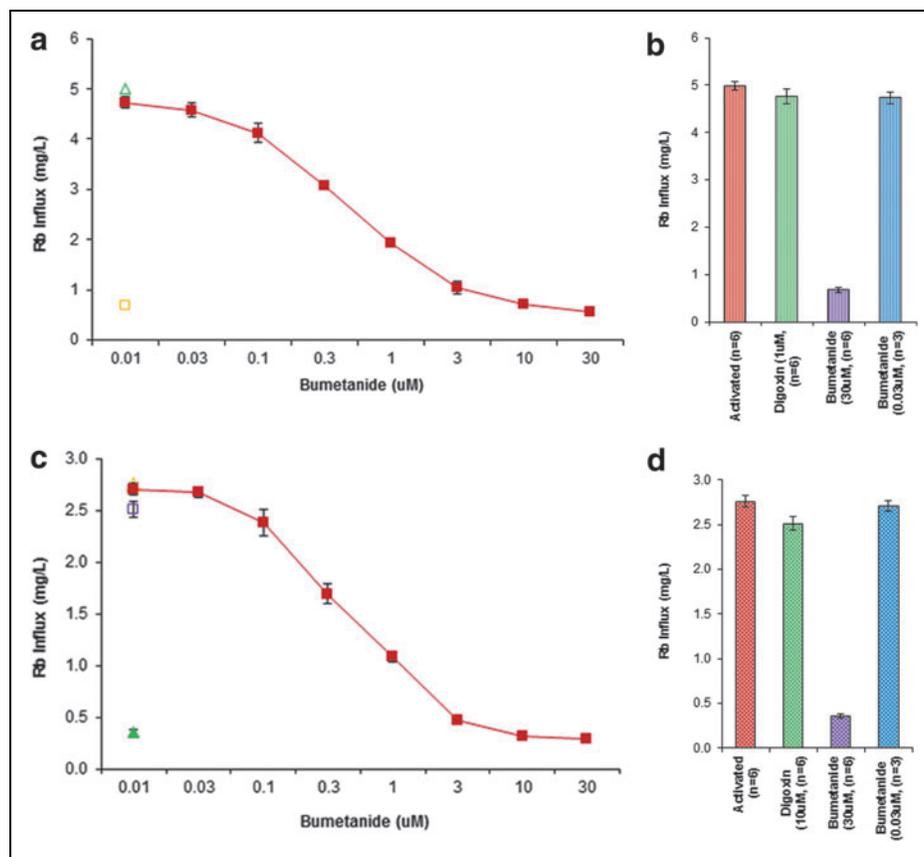
Optimization of Window of Detection

To further optimize the detection window, the following experiments were carried out and optimization profile is presented in *Table 2*.

(a) Cold treatment during wash step: The active kinetics of NKCC1 could contribute to intracellular Rb$^+$ content because of its basal activity at room temperature in addition to the basal activity of Na$^+$,K$^+$-ATPase. This contribution could be decreased by lowering the kinetics of the basal influx by using wash buffer at 4°C. As expected, the cold buffer treatment resulted in a significant rise in the window of detection from 2.6- to 5.9-fold with a basal influx of 17% during 3 min activation (*Fig. 1d*).

(b) Strengthening of extracellular Rb$^+$: It was thought that raising Rb$^+$ concentration in the activation influx buffer could increase its contribution to the intracellular Rb$^+$ content by influencing the amount of Rb$^+$ entering through the NKCC1 in open state. Indeed, the raising of Rb$^+$ from 2.5 to 5.4 mM in the activation buffer led to an increase in the window of detection from 5.9-fold to 8.4-fold during 3 min activation (*Fig. 2a*). The total amount of Rb$^+$ uptake was found to be 4.9 ng/μL. The Rb$^+$ influx generated from this experiment indicated that the complete blocking dose of digoxin was 10 μM. This resulted in only 5% of the total Rb$^+$ influx through the Na$^+$,K$^+$-ATPase, whereas the highest (30 μM) dose of bumetanide inhibited 86% influx through the NKCC1 (*Fig. 2b*).

(c) Optimization of activation duration: To further minimize the contribution of Na$^+$,K$^+$-ATPase to the total Rb$^+$ uptake, another tweaking attempt was made by reducing the duration of activation from 3 to 2 min. This resulted in an apparent decrease of the total Rb$^+$ uptake from 4.9 to 2.8 ng/μL (*Fig. 2c*). This experiment indicated that the 10 μM digoxin was still the complete blocking dose of Na$^+$,K$^+$-ATPase. This also showed that only 9% of the total Rb$^+$ influx was through the Na$^+$,K$^+$-ATPase, whereas the highest (30 μM) dose of bumetanide inhibited 87% through the NKCC1

Fig. 2. **(a)** Dose response curve of bumetanide on Rb^+ influx activated in the presence of 5.4 mM of RbCl in the activation buffer for 3 min in the presence of 10 μM of digoxin (■). Positive control 30 μM of bumetanide (□) and negative controls: activated Rb^+ influx in the absence (△ hidden behind ■) and presence of 10 μM of digoxin (▲). The rise in the extracellular concentration of Rb led to an increase in the window of detection to 8.4-fold. **(b)** Comparison of Rb^+ influx (mg/L) activated for 3 min in the presence of 5.4 mM RbCl in the activation buffer for 3 min with 10 μM of digoxin, and nonblocking (0.01 μM) and full-blocking (30 μM) doses of bumetanide. This indicated 10 μM of digoxin as a complete blocker of Na^+, K^+, ATPase, whereas the highest (30 μM) dose of bumetanide inhibited the NKCC1. **(c)** Dose response curve of bumetanide on Rb^+ influx activated for 2 min instead of 3 min in the presence of 10 μM of digoxin (■). Positive control 30 μM of bumetanide (▲) and negative controls: activated Rb^+ influx in the absence (△) and presence of 1 μM of digoxin (□). The 2 min activation generated higher window of detection than 3 min activation. **(d)** Comparison of Rb^+ influx (mg/L) activated for 2 min in the presence of 10 μM digoxin, and nonblocking (0.01 μM) and full blocking (30 μM) doses of bumetanide. **(e)** Comparative ratio indicated higher window of detection during 2 min of activation. Error bars represent standard error of $n = 3–6$ values. **(f)** Dose response of bumetanide with activation duration of 2 min on induced (■) and uninduced (▲) expression of NKCC1 in the absence of any blocker of Na^+, K^+-ATPase, suggesting that addition of Na^+, K^+-ATPase blocker to the assay is not necessary to maintain a high window of detection (8.2 to 9.5). **(g)** Comparison of Rb^+ influx (mg/L) activated for 2 min showing induced and uninduced conditions with its full block by bumetanide, respectively. **(h)** Comparison of window of detection of both the induced and uninduced NKCC1, suggesting the contribution of the inducer in the assay. Error bars represent standard error of $n = 3$ values. **(i)** Variability among the entire 96-well plate showing activated (*Row* 1, ◇; *Row* 2, ■; *Row* 3, ▲; and *Row* 4, □) and basal Rb^+ influx (mg/L) activated (*Row* 5, ✗; *Row* 6, •; *Row* 7, ◇; and *Row* 8, △) for 2 min. **(j)** Comparison of window of detection determined by activated and basal influx providing supportive evidence to its robustness. Error bars represent standard error of $n = 48$ values. *Continued.*

(*Fig. 2d*). Under this optimization step, the activation duration of 2 min generated higher window of detection than that of 3 min (*Fig. 2e*).

(d) Elimination of Na^+, K^+-ATPase inhibitor from test compound screen: The Rb^+ uptake by Na^+, K^+-ATPase is known to be significantly low during initial duration of 2 min.[15] It was also supported by the results from the previous experiment involving NKCC1 activation for

2 min. Therefore, to eliminate the presence (interference) of the Na^+, K^+-ATPase inhibitor in the screen, the dose response of bumetanide was attempted on NKCC1 in the absence of any blocker of Na^+, K^+-ATPase. The results indicated that the absence of Na^+, K^+-ATPase blocker did not affect the window of detection; rather, it lead to an apparent increase (from 8.4 to 9.5) in the fold of window of detection (*Fig. 2f*).
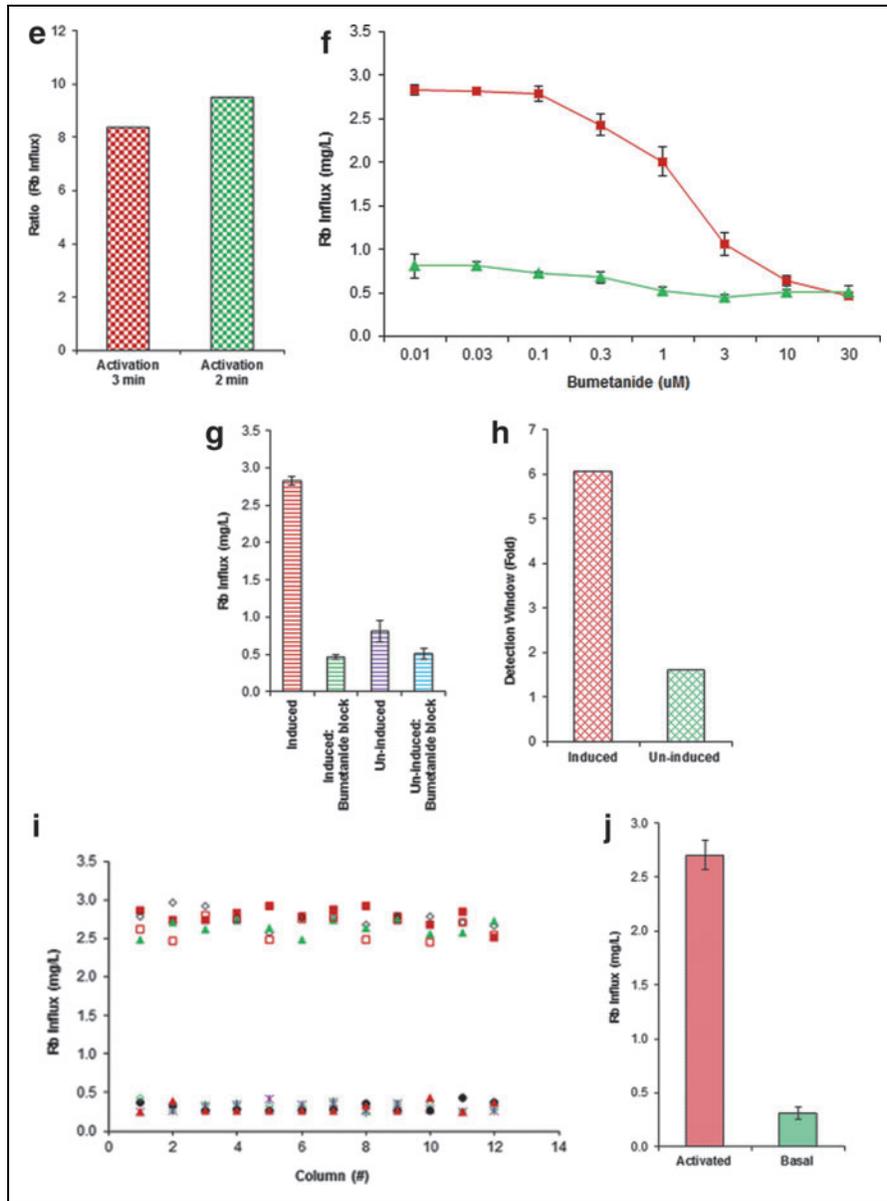
Fig. 2. (*Continued*)

Table 3. IC$_{50}$ Rank Order of Test Compounds

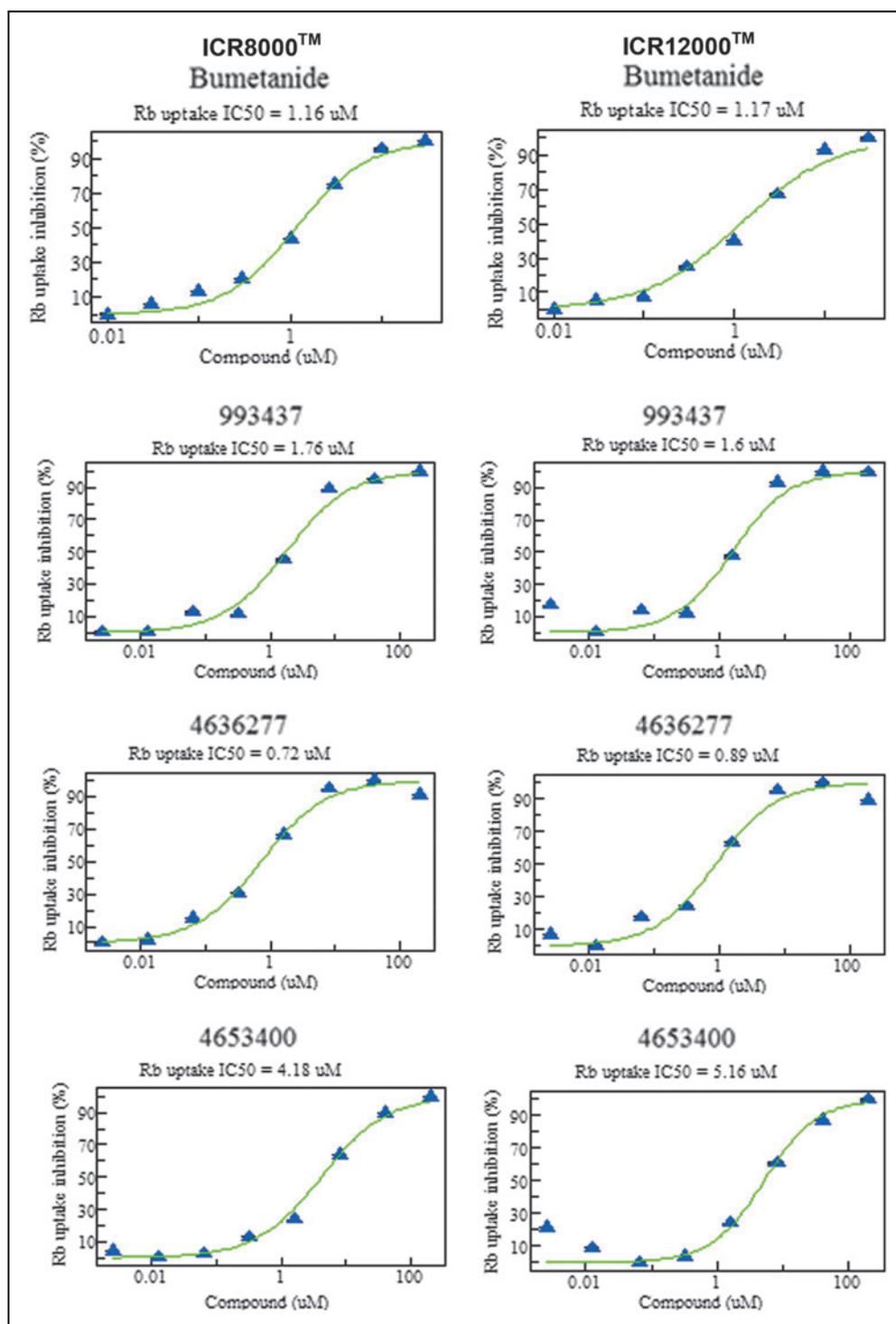| Test compound	ICR8000 IC$_{50}$ (μM)	ICR12000 IC$_{50}$ (μM)	Rb^{86} IC$_{50}$	Rb^{86} rank order	ICR8000 rank order	ICR12000 rank order
4636277	0.72	0.89	0.3	1	1	1
Bumetanide	1.16	1.17	1.5	2	2	2
993437	1.76	1.6	5.9	3	3	3
4653400	4.18	5.16	12.0	4	4	4

Fig. 3. IC$_{50}$ rank order of test compounds.

Comparison of Induced and Uninduced NKCC1 Expressed in HEK Cells

The objective of this experiment was to compare the Rb$^+$ influx in the NKCC1 expressing cells under both the induced and uninduced conditions. The NKCC1 was activated for 2 min in the presence of 5.4 mM of RbCl in extracellular activation buffer. Under these conditions, the dose response of bumetanide was evaluated in the absence of any inhibitor of Na$^+$,K$^+$-ATPase. It was found that even under the uninduced conditions, the NKCC1 allowed bumetanide-sensitive influx of Rb$^+$ (*Fig. 2g*). However, the maximum Rb$^+$ influx in the uninduced cells was 28.6% of the induced condition. The total Rb$^+$ influx in case of induced condition was 3.8-fold higher than that of the uninduced condition. Bumetanide (10 µM) could block 84% of the induced Rb$^+$ influx, leading to a window of detection of sixfold. This dose of bumetanide could block only 37% of the total Rb$^+$ influx during the uninduced condition with 1.6-fold window of detection (*Fig. 2h*).

Variability and Robustness

One of the critical features of such an assay is its ability to prove its robustness. An 8.7-fold window of detection of this assay for the NKCC1 was a valuable measure for running an HTS. The robustness of the assay was determined by calculating the Z′, a statistical function used to evaluate the robustness of an HTS.[24] This factor takes into consideration the standard deviation among the replicates as well as the window of detection (mean of high values – mean of low values). In the present assay, the Z′ value was calculated for the entire plate, wherein 48 wells were activated and the remaining 48 wells were unactivated, thus representing basal influx of Rb$^+$ (*Fig. 2i, j*). The Z′ value of >0.9 indicated that
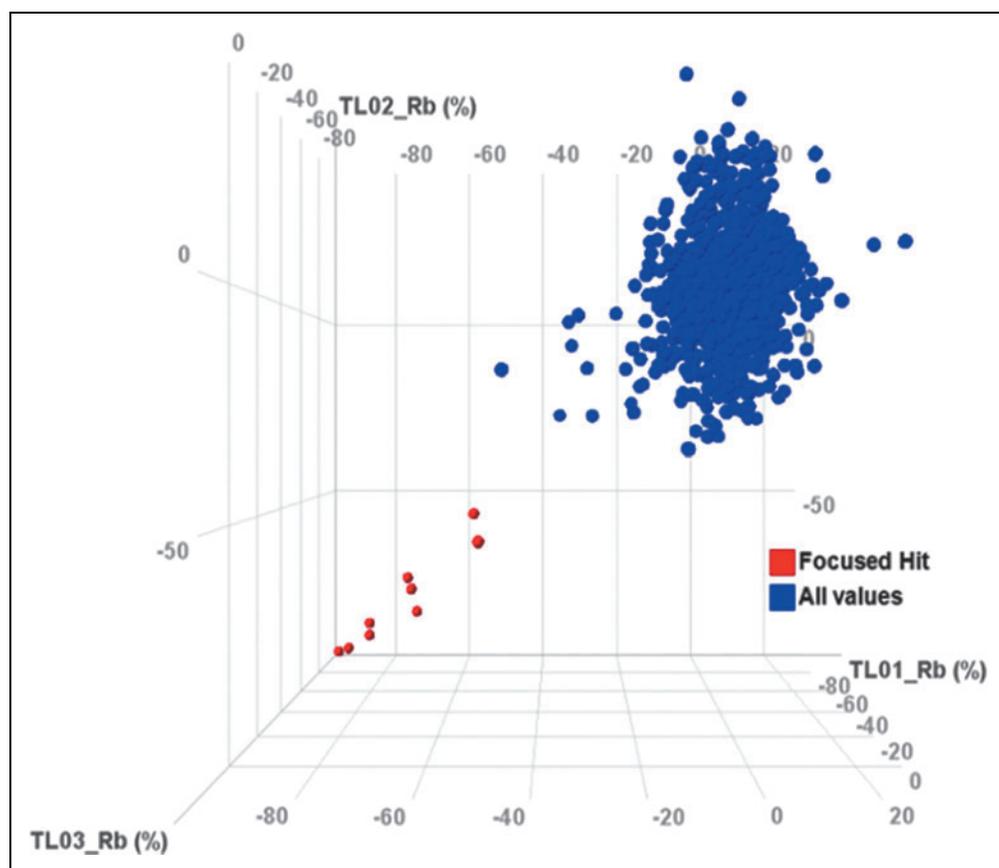
Fig. 4. Focused library correlation, 0.7% hit rate at 40% cut-off (focused hit, all values), suggesting Rb$^+$ influx assay as a robust and effective screen in 384-well format.

focused library of 1450 compounds in three independent runs. Robust results were achieved with a Z$'$ >0.7 and very good correlation among the three independent runs in the automated assay (*Fig. 4*). A full HTS of 1.2 million compounds was followed. Chemical classes of specific hits were generated with dose response confirmation from the Rb$^+$ influx assay. A counter screen Rb$^+$ influx assay on the wild-type cells was also carried out for comparison with Rb$^+$ entry routes through other endogenous ion channels and cotransporters.

Assay Advantages

The Rb$^+$ flux assay is capable of detecting Rb$^+$ in the intracellular and extracellular samples with sensitivity >0.07 µg/L, thus providing greater confidence in the drug discovery process. Although an end point assay, the Rb$^+$ tracer flux approach is high throughput while offering high sensitivity, specificity, simplicity, miniaturization, workflow optimization, and amenability to automation. This cell-based Rb$^+$ flux assay has multiple advantages over other existing technologies.

Traditional gold standard electrophysiology techniques including manual patch and automated patch clamping suffer from their inherent issues of high cost and being too slow and applicable to individual cell to be compatible in high-throughput format. Being electroneutral, the NKCC1 are a difficult target for electrophysiology techniques. In contrast, the cell-based Rb$^+$ flux assay involves a population of cells per well that reflect a response as a significant mean of multicellular responses versus a selected cell in patch clamp.[16]

In addition, the assay does not suffer from artifacts associated with fluorescent assays for ion channels and cotransporters because it is a flux-based functional assay carried out in the presence of simple and nonfluorescent salt solutions. The fluorescence-based Tl$^+$ assay, for example, suffers from cytotoxicity concerns because it involves the halide-sensitive nonfluorescent FluxOR™ dye loading into cells. Thus, the

the assay had high window of detection along with significantly low standard deviation among the replicates ($n = 48$) in a 96-well plate. For cell-based assays, a Z$'$ of 0.5 is usually the lower limit of acceptance for an HTS.[21,22]

Testing of Blind Compounds

The optimized conditions for the Rb$^+$ influx assay were employed in testing a set of blind compounds using both ICR series ICR8000 and ICR12000. The IC$_{50}$ determinations and their rank order are presented in *Table 3*. The IC$_{50}$ curve fits with typical curvatures and display insignificant SEM error bars, showing the quality of the assay (*Fig. 3*). The rank order determined by ICR8000 matched that of the high-throughput system ICR12000, which was also supported by the ^{86}Rb$^+$ flux assay.

HTS Campaigns

This Rb$^+$ influx assay was further optimized into 384-well format and used first to screen for NKCC1 inhibitors with a

exclusion of the halides from cells in performing this assay turns out to be nonphysiological. The activity of NKCC1 is strongly dependent on its phosphorylation in its regulatory domain; therefore, absence of cell chloride concentration in chloride-free buffers used in such assays affects its activity.[25] The cytoxocity concern is also supported by the fact that the Tl^+-sensitive indicator is cleaved from the FluxOR dye inside the cell after the dye is loaded into the cells for about 1 h. The water-soluble probenecid acid meant to stop the extrusion of the Tl^+-sensitive derivative from the cells blocks organic anion pumps that raise additional concerns (FluxOR Potassium Ion Channel Assay Life Technologies; Catalog nos. F10016 and F10017). Moreover, the Tl^+ assay also takes a long time as the dye-loading step is 1 h at 37°C, and thus cells are exposed to this reagent for a long time. Tl^+ being a potent carcinogen, its exposure to laboratory personnel may also prove dangerous.[26,27]

The HTS for ion channels and transporters is normally carried out in native or heterologous cell-based systems that suffer from interference from other endogenous channels and transporters that may result in false-positive or false-negative hits.[28] For the purpose of screening such targets free from these interferences, a novel technology using cell-free synthetic vesicles (liposomes) incorporated with target ion channels or transporters along with tracer ion may be employed.[28–30]

CONCLUSION

The new functional assay we describe here is extremely useful in HTSs and for characterization of novel NKCC1 modulators. This nonradioactive Rb^+ flux assay coupled with ICR8000 or ICR12000 provides a system to work with NKCC1 in determining confident and concordant rank orders of the test compounds in an HTS format. Detection of nonradioactive Rb^+ tracer with the ICR series can be reliably used in drug discovery of antagonists, and to study the functional activity of NKCC1. The determination of excellent values for the Z' of the Rb^+ flux assay also suggests that the assay is robust and sensitive not only for ion channels but also for cotransporters such as Na^+,K^+-ATPase and NKCC1. As the ICR8000/ICR12000 is equipped with an automated sampling device with microliter sampling technology, it provides the capability for screening compounds in HTS format.

ACKNOWLEDGMENT

DISCLOSURE STATEMENT

REFERENCES

1. Cong D, Zhu W, Kuo SJ, et al.: Ion transporters in brain tumors. *Curr Med Chem* 2015;22:1171–1181.
2. Orlov SN, Koltsova V, et al.: NKCC1 and NKCC2-The pathogenetic role of cation-chloride cotransporters in hypertension. *Genes Dis* 2015;2:186–196.
3. Carmosino M, Rizzo F, Torretta S, et al.: High-throughput fluorescent-based NKCC functional assay in adherent epithelial cells. *BMC Cell Biol* 2013;14:16–25.
4. Isenring P, Jacoby SC, Chang J, et al.: Mutagenic mapping of the Na-K-Cl cotransporter for domains involved in ion transport and bumetanide binding. *J Gen Physiol* 1998;112:549–558.
5. Weaver CD, Harden D, Dworetzky SI, et al.: A thallium-sensitive, fluorescence-based assay for detecting and characterizing potassium channel modulators in mammalian cells. *J Biomol Screen* 2004;9:671–677.
6. Zaarour N, Defontaine N, Demaretz S, et al.: Secretory carrier membrane protein 2 regulates exocytic insertion of NKCC2 into the cell membrane. *J Biol Chem* 2011;286:9489–9502.
7. Terstappen GC, Roncarati R, Dunlop J, et al.: Per Screening technologies for ion channel drug discovery. *Future Med Chem* 2010;2:1–16.
8. Yu H, Li M, Wang W, et al.: High throughput screening technologies for ion channels. *Acta Pharmacol Sin* 2016;37:34–43.
9. Zou B, Yu H, Joseph JB, Chanda P, et al.: Profiling diverse compounds by flux- and electrophysiology-based primary screens for inhibition of human *Ether-à-go-go* related gene potassium channels. *Assay Drug Dev Technol* 2010;8:743–754.
10. Hoffmann EK, Lambert IH, Pedersen SF: Physiology of cell volume regulation in vertebrates. *Physiol Rev* 2009;89:193–277.
11. Flatman PW: Cotransporters, WNKs and hypertension: important leads from the study of monogenetic disorders of blood pressure regulation. *Clin Sci* 2007;112:203–216.
12. Zeuthen T, Macualay N: Cotransport of water by Na^+-K^+-$2Cl^-$ cotransporters expressed in Xenopus oocytes: NKCC1 versus NKCC2. *J Physiol* 2012;90:1139–1154.
13. Susa K, Kita S, Iwamoto T, et al.: Effect of heteozygous deletion of WNK1 on the WNK-1/SPAK-NCC/NKCC1/KNCC2 signal cascade in the kidney and blood vessels. *Clin Exp Nephrol* 2012;16:530–538.
14. Nancy D, Mercado MA, et al.: Gain-of-function missense variant in SLC12A2, encoding the bumetanide-sensitive NKCC1 cotransporter, identified in human schizophrenia. *J Psychiatr Res* 2016;77:22–26.
15. Gill S, Gill R, Wicks D, et al.: Development of an HTS assay for Na^+,K^+-ATPase using non-radioactive rubidium ion influx. *Assay Drug Dev Technol* 2004;2:535–542.
16. Gill S, Gill R, Xie Y, et al.: Development and validation of HTS flux assay for endogenously expressed chloride channels in a CHO-k1 cell line. *Assay Drug Dev Technol* 2006;4:65–71.
17. Gill S, Gill R, Wicks D, et al.: A cell-based Rb^+-flux assay of the Kv1.3 potassium channel. *Assay Drug Dev Technol* 2007;5:373–380.
18. Rezazadeh S, Hesketh JC, Fedida D: Rb^+ flux through hERG channels affects the potency of channel blocking drugs: correlation with data obtained using a high-throughput Rb^+ efflux assay. *J Biomol Screen* 2004;9:588–597.
19. Sorota S, Zhang XS, Margulis M, et al.: Characterization of a hERG screen using the IonWorks HT: comparison to a hERG rubidium efflux screen. *Assay Drug Dev Technol* 2005;3:47–57.
20. Clay WS, Deidre EW, Trivedi S, et al.: Medium-throughput functional assay of KCNQ2 potassium channels using rubidium efflux and atomic absorption spectrometry. *Anal Biochem* 2003;319:251–257.

21. Wang K, Mcilvain B, Tseng E, *et al.*: Validation of an atomic absorption rubidium ion efflux assay for KCNQ/M-channels using the Ion Channel Reader 8000. *Assay Drug Dev Technol* 2004;2:525–534.

22. Trivedi S, Dekermendjian K, Julien R, *et al.*: Cellular HTS assays for pharmacological characterization of Na$_V$1.7 modulators. *Assay Drug Dev Technol* 2008;6:167–179.

23. Jinlong Q, WangY, LiuY, *et al.*: Development and validation of HTS assay for screening the calcium-activated chloride channel modulators in TMEM16A stably expressed CHO cells. *Anal Bioanal Chem* 2014;406:1713–1721.

24. Zhang JH, Chung TD, Oldenburg KR: A simple statistical parameter for use in evaluation and validation of high throughput screening assays. *J Biomol Screen* 1999;4:67–73.

25. Hannemann A, Flatman PW: Phosphorylation and Transport in the Na-K-2Cl Cotransporters, NKCC1 and NKCC2A, Compared in HEK-293 Cells. PLoS One 2011;6:1–9.

26. Saddique A, Peterson CD: Thallium poisoning: a review. *Vet Hum Toxicol* 1983;25:16–22.

27. Cvjetko P, Cvjetko I, Pavlica M: Thallium toxicity in humans. *Arh Hig Rada Toksikol* 2010;61:111–119.

28. Gill S: Development of high throughput screening technology using synthetic lipid vesicles and ion channel reader (abstract of presentation). *Ion Channel Retreat Report* 2008:P 43.

29. Choy N, Davis A, Brugger S, *et al.*: Review-The sixth annual Ion Channel Retreat Vancouver, Canada, June 23–25, 2008. *Assay Drug Dev Technol* 2008;6:759–764.

30. Su Z, Brown EC, Wang W, *et al.*: Novel cell-free high throughput screening method for pharmacological tools targeting K+ channels. *Proc Natl Acad Sci U S A* 2016;113:5748–5753.

Address correspondence to:
Sikander Gill, PhD
Aurora Biomed Inc.
1001 E Pender Street
Vancouver V6A 1W2
British Columbia
Canada

E-mail: info@aurorabiomed.com

Abbreviations Used

HEK	= human embryonic kidney
HTS	= high-throughput screen
ICR	= Ion Channel Reader